DIELECTRIC AND COMBINED NMR/CAPILLARY PRESSURE METHODS FOR MONITORING LIQUID/AIR AND LIQUID/LIQUID INTERFACE EVOLUTION: APPLICATION TO ROCK AND MINERAL WETTABILITY STUDIES

Ben Clennell, Artem Borysenko, Iko Burgar, Rossen Sedev, John Ralston
CSIRO Petroleum, 26 Dick Perry Ave, Kensington, WA 6151, Australia
Ian Wark Res. Inst., University of South Australia, Mawson Lakes, SA 5095, Australia

This paper was prepared for presentation at the International Symposium of the Society of Core Analysts held in Calgary, Canada, 10-12 September 2007

ABSTRACT

We used complementary petrophysical methods to monitor time evolution of liquid/air and liquid/liquid interfaces in porous media. Real and imaginary dielectric constants versus frequency (10 MHz - 3 GHz) were recorded for samples at different levels of water saturation using a 6 mm diameter coaxial probe. Since the full frequency sweep takes only around 10 seconds, dielectric measurements can be used to study very fast processes following immediately from introducing a new fluid to the powder pack. We also used measurements of dielectric loss over periods of hours to study clay hydration and swelling.

A low field (2 MHz) NMR spectrometer was used to monitor changes in the proton transverse relaxation (T_2) spectra of the fluid phases using the CPMG pulse sequence repeated at regular intervals. High field NMR instrument (300 MHz) were used to investigate surface adsorbed species using Magic Angle Spinning (MAS) proton and carbon NMR spectroscopy and low field (20 MHz) proton NMR signal using Free Induction Decay (FID). We investigated model systems of pure minerals and powdered shales whose physical properties and mineralogy have been thoroughly investigated. Powder packs were tested in the original state, and after aging with crude oil.

During the NMR experiments we could observe differences in shapes of CPMAS and DDMAS spectra enabling us to follow the fluid distribution within porous medium depending on shale hydrophobicity. Changes in the short T_2 component can be related to the physicochemical processes of adsorption and swelling. Subsequent FID measurements made at 20 MHz resonant frequency show that oil-aged minerals have different amounts of surface adsorbed fluids, and these relax at widely different rates.

These observations confirmed our interpretations of the petrophysical responses concerning which shales are hydrophilic and which have a tendency to adsorb oil and even become oil wet. The findings are consistent with measurements of wetting and swelling tendencies of the powders and intact shales that we conducted using standard methods. These results give us confidence that a combination of petrophysical

measurements holds promise for rapid laboratory assays of wettability in more complex natural systems.

INTRODUCTION

As it has been shown in our companion paper (Borysenko et al. 2007) there are several parameters that can be considered as a criterion of rock wettability. However in some cases such as wettability of mudrocks (Borysenko et al. 2006), the study of liquid adsorption and removal from the solid surface is very important. Therefore an effective, non-destructive method of monitoring is required to assess various aspects of fluid-rock interaction. High resolution methods such as environmental scanning electron microscopy (ESEM), atomic force microscopy (AFM) are valuable to directly probe mineral surfaces and identify adsorbed species, but these methods are less useful when we attempt to understand processes occurring throughout a porous medium under dynamic conditions of fluid displacement. We have therefore been using NMR spectroscopy and dielectric measurements to assess liquid/solid interaction and liquid mobility within porous space of a model rock composed of packed powdered shale, clay or quartz sample (Borysenko 2007). Both of dielectric methods (Garrouch et al. 1994, Bona et al. 1998, Nguyen et al. 1999) and NMR methods (Zhang et al. 2000, Al-Mahrooqui et al. 2003, Fleury et al. 2003, Looyestijn and Hofman 2005, Djurhuus et al. 2006) have a long track record in rock wettability research but they have rarely been used in combination, and few studies have been conducted specifically on clays and shales.

SAMPLES

To characterise the conditions of liquid/liquid/solid and/air/liquid/solid interface formation in model systems and natural shales we varied the water saturation in a controlled manner. The model systems we chose are quartz silt, Q, montmorillonite clay, M, kaolinite, K, and a mixture of 90% quartz with 10% of the montmorillonite, QM). Quartz silt was thoroughly cleaned and washed, to produce a powder that is strongly water wet. A batch of this clean quartz was subjected to a surface treatment to add a methyl group that renders it hydrophobic: the methylated quartz was washed again to remove excess reagent. To explore the effects of natural wettability variation we chose two shales from Australia that represent end members from a previously screened set of samples (the results are described in the companion paper **A14**). Shale O1A, from the Bass Basin, contains quartz and kaolin and is hydrophobic. The other shale L1_390, from the continental Lancer Basin, contains abundant illite and is strongly hydrophilic. We tested the shales in an "original" state of preserved water content (taken from the drill core and stored under oil), and also in a dried and powdered form. We could verify that the interior part of the preserved shales was not affected by the storage oil by using fluorescence microscopy on the surfaces of broken fragments when we split open a sub-sample. The use of a powder enabled us to access a large internal surface of the multimineralic shales without extraordinarily high capillary pressures. To study the changes in wettability after interaction with crude oil we tested the quartz silt, clay and powdered shales before and after a simplified aging process. Dupuy Crude from Western Australia and lighter crude from South Australia were used.

DIELECTRIC METHODS

One characteristic of porous media which is strongly affected by fluid mobility and distribution is the dielectric constant. Our dielectric measuring system consists of a Vector Network Analyzer (Agilent ENA 5071B) and a coaxial probe (end-loaded transmission line) 6 mm in diameter that is placed against the sample to be tested. A swept frequency of 10 MHz to 3 GHz is used. Software returns both the real part of the relative permittivity (dielectric constant) and the imaginary relative permittivity, or dielectric loss of the test material in the sensed volume. The imaginary part of the dielectric constant - dielectric loss depends mainly on ohmic conductivity. Samples with higher water content are less resistive (more dielectric loss) than samples with low water content. To calculate conductivity from loss one multiplies the value by the frequency, and by the constant permittivity of vacuum (ε_0):

$$\sigma = 2\pi \cdot \varepsilon_0 \cdot f \cdot e''$$

where σ conductivity determined at frequency f.

In a series of simple tests to demonstrate the method, we started with the dry powder (clay mineral or powdered shale, pretreated, aged or not) and added water drop-wise to around 80% of saturation. After each step of hydration we measured the weight change with a balance and a new dielectric spectrum was acquired. Several minutes were allowed for equilibration in each step and in some cases we repeated measurements again after some hours or overnight.

RATIONALE FOR DIELECTRIC METHODS

Water has a high dielectric constant (79) compared with mineral grains or oil (about 4-5). At high frequency the dielectric constant values reflect mainly the amount of water compared with air, solids and oil, according to a volumetric mixing law.

Values of rock dielectric constant > 80 are possible at low frequency even though none of the solid or fluid constituents have dielectric constants that high. This dielectric enhancement at MHz to kHz frequency comes from electrical polarization of rock-fluid and fluid-fluid interfaces. Surface active, clay-rich samples and samples with multiple fluid films show greater dielectric enhancement. Water bound to clays can to some extent 'short circuit' the bulk water conductivity signal, and increase the overall conductivity per unit of water content, as well as increasing the relative permittivity over that of clay-free samples. Where the sample is known to contain clays but the enhanced dielectric permittivity in the 10-100 MHz region is suppressed or absent, it gives us a good indication that oil is directly adsorbed onto most of the mineral grains, shutting off the enhanced surface polarization and conductivity associated with clay-water interfaces. Where the water phase is discontinuous ohmic conductivity is low, and the spectrum typically shows a dielectric loss that is more important at high frequency (GHz range) where dipolar molecular relaxation occurs.

NMR METHODS

The most straightforward analysis method is determination of the bulk sample transverse

nuclear spin relaxation time (T_2) decay which was obtained with a low field NMR spectrometer (2 MHz Maran Ultra) using the CPMG pulse sequence in a uniform magnetic field. A conventional regularized least-squares inversion routine was used to invert the decaying echo train to a T_2 spectrum. In the Maran instrument the initial echo signal is detected after an interval of around 250 μs, and with 230μs inter-echo spacing, so only protons in fluids with a spin lifetime of tens of μs are detected. Practically, that means that liquids in pores of all sizes down to nm size are detected, together with some fluid bound to surfaces, but protons bound to surfaces and within solid phases are not detected.

To investigate the oil and water molecules and other protonated or carbon-bearing groups at the surface itself or in the solid state we used several methods of solid state NMR spectroscopy on the samples in their original state, after surface methylation or aging treatments, and after oil/water exposure. ^{13}C NMR measurements were made using a Varian 300 MHz spectrometer. High-resolution solid-state ^{13}C NMR spectra were obtained by the combined use of cross polarization and magic-angle spinning (CPMAS) and without CP – only with ^{1}H high-power dipolar decoupling (DDMAS). We also conducted simple proton Free Induction Decay, CPMG and Solid Echo measurements at 20 MHz in a Bruker Minispec PC120 with a short dead time of 25 μs. The solid echo sequence uses two pulses, and the data is recorded with time = 0 commencing after the first pulse. FID data are fitted to a simple model with Gaussian and exponentially decaying components reflecting protons in solids, at surfaces and protons in the fluid phases.

RATIONALE FOR NMR METHODS

The low field (2 MHz Maran) NMR methods probe a sample volume of 20-70 cm^3 and require about 1-5 g of hydrogen-bearing liquid in the sample to produce reliable results. The main advantage of low fields is relative insensitivity to the magnetic susceptibility contrasts of grains and matrix that are problematic in real rocks. On the other hand, the higher resolution NMR techniques CPMAS and DDMAS have enormously higher signal to noise ratio and are sensitive to micrograms or even nanograms of the target compounds (bearing ^{1}H or ^{13}C nuclei) so they can respond to monolayers or the presence of surface species. For example, we can detect the methyl groups we added by chemical treatment to make the silicate surfaces hydrophobic. These two solid-state NMR methods have been used extensively for solid organic matter and coal analysis (Song et al. 1994) , but have not apparently been applied much in the context of wettability studies. The FID and Solid Echo pulse sequences together provide a very robust method both for detecting surface compounds and the bulk fluids and distinguishing their different relaxation rates. The Solid Echo method is usually used for detecting only nuclei in the solid phase with no fluids present in the sample. We have used the Solid Echo sequence to enhance the signal from solid phase nuclei, but the mobile or liquid signal is little attenuated, and so in the recorded data we can see very early decaying nuclei in liquid molecules residing close to surfaces too. CPMG at 20 MHz with the Minispec gives superior signal to noise and shorter dead time compared with the 2MHz CPMG acquisition in the low-field Maran instrument.

RESULTS

Hydrophobic/Hydrophilic Nature of Clay Types and Response to Aging

Considering the hydration of L1_390 shale samples preserved under oil (storage oil Shell P-874 containing alkanes and napthenes) using optical microscopy we could see a dramatic change in the surface texture as a result of hydration and after slaking as a result of oil displacement by water (Fig. 1). The fast formation of a multitude of cracks and slaking is accompanied by decrease of the contact angle. Fig. 2 shows the time evolution of the water in air contact angle from 130° before the surface oil film ruptured, to an ultimate value of 40°. Considering now the effect of different natural oils on clay powders, we can see that the chemical content of crude oil has a strong effect on the rate of wettability restoration following aging. The evolution from a hydrophobic to hydrophilic state occurs faster for clays aged in lighter crude oil from Cooper Basin (South Australia) than for the Dupuy Crude (WA). After aging in both oils, kaolinite clay powder (K), which is more hydrophobic, exhibits a higher contact angle and this remains higher value in comparison to montmorillonite clay powder (M).

Dielectric Measurements on Aged and Hydrated Samples

The results of dielectric constant measurements for quartz powder (<10 μm size) treated crude are presented in Fig. 3. The sample has a very low and non-dispersive dielectric constant and the dielectric loss is too small to be measured reliably: there is no conductive film of water adsorbed from the air. With progressive hydration the dielectric constant increases, but low frequency interfacial dispersion is more important at low water content (where air-water and oil-air interfaces are present), than when fully saturated. The water saturation leads to increase of ε' and ε'' values. However, after further water injection, we could see leveling-off in dielectric loss over the frequency range.

If we consider the conductivity for samples gradually saturated with water, presented in Fig. 3c, we can see that samples show dispersion of the real dielectric constant with frequency and a concomitant increase in conductivity as frequency increases. Flatter conductivity trends are indicative of less dispersion and a less important contribution from charged interfaces to the electrical signature. At the highest frequencies, the apparent conductivity (Fig. 3c) is influenced by water dipolar loss: this component of apparent conductivity increases with water content irrespective of whether that water is connected or not. On the other hand, the conductivity due to ohmic conduction through the sample requires that the water phase is connected.

The hydrophilic shale L1_390 shows higher conductivity in comparison to hydrophobic sample O1A. This is likely due to a more significant component of conduction in the clay bound water relative to that in the pore space fluids. An interesting result was found for hydrophobic shale where the trend of increasing (low frequency) conductivity with increasing water content leveled off at quite modest water contents. We surmise that trapped air blocked the establishment of efficient conduction pathways through the inter-aggregate pore water. Additional water-because of surface repulsion-did not reach the pore throat regions and small pores needed to make continuous pathways.

NMR Results

Figure 4 gives two examples of time-lapse CPMG acquisitions of proton T_2 spectra obtained with the CPMG pulse sequence in the low-field 2MHz Maran instrument. In the first example (Fig 4a) water flows into a clean quartz pack by spontaneous imbibition. At time = 0 there is 8 ml of water in the sample, and more is allowed to flow in spontaneously over 240 minutes, as T_2 spectra are acquired periodically. After 240 minutes oil is injected by forced imbibition using a syringe pump, with increments of 2ml followed by equilibration periods. After each equilibration period a new spectrum is acquired. The distinct peaks for oil and water can be seen as the system readjusts to the fluid content changes. In the second example (Fig. 4b) we see in the changing T_2 distribution the rearrangement of water over time during progressive forced imbibition into a model shale system consisting of 90% quartz and 10% montmorillonite clay. In this case the distinct peaks are clay-bound water (around 1 ms T_2) and the inter-granular pore water ($T_2 > 50$ ms).

Figure 5 gives examples of 20MHz Minispec solid echo data for two shale samples both clean and aged in crude oil. The baseline signal in clean shales is relatively large, and comes from clay bound water. In O1A the clay bound water shows a Gaussian curve shape restricted to short times, whereas for the hydrophilic shale the water layer can be assumed to be thicker as the spin lifetime is longer and the decay of an exponential nature. (Note for clean quartz-not shown here- the baseline solid echo curve is near zero: there is nothing adsorbed on the surfaces that contains protons). The additional signal in the aged shale samples is from oil compounds adsorbed in the aging process. The distribution of these is different in the two shales, with the hydrophobic shale showing two distinct components. However, from solid echo we cannot tell much more than this. We must use e.g. high resolution NMR methods to discern the details of what species are adsorbed and how they bond to surfaces.

Figure 6 shows the proton broad line spectrum for clean quartz compared with methylated quartz. The methylation process adds a proton-bearing group to the quartz surface which is detected at extremely small mass concentrations. The background signal on clean quartz must come from (protons in) water adsorbed on the quartz from the air.

Figure 7 shows the ^{13}C CPMAS NMR spectra for the two shales again obtained using the Varian high field instrument for solid state measurements, but tuned to detect carbon 13 rather than proton resonance. The untreated hydrophobic shale O1A does have a small signal, suggesting that the hydrophobicity could relate to small amounts of organic carbon on the surface (untested hypothesis). The hydrophilic shale L1_390 is basically free of carbon, and adsorbs less distinctly the oil components during aging. The samples aged in oil have distinct spectra, though signal to noise appears rather poor with this method. On the other hand, the DDMAS results for the same samples (Fig 8.) show excellent spectral resolution of multiple components.

CONCLUSIONS AND OUTLOOK

Our results to date are proof of concept that dielectric and NMR methods demonstrated for reservoir rocks can be applied also to clays and shales. The high field NMR methods we tested here show promise to compliment the low field methods that most previous work has focused on, though of course there is not the same direct applicability to the downhole environment.

Dielectric tools have been developed for the oilfield in the past, and despite a number of studies, including this one that shows their usefulness for wettability monitoring in the lab, there are few field applications as yet. This picture may well change as a new generation of electrical logging tools operating at frequencies well beyond 1 MHz become available.

REFERENCES

Al-Mahrooqi, S. H.; Grattoni, C. A.; Moss, A. K.; Jing, X. D., An investigation of the effect of wettability on NMR characteristics of sandstone rock and fluid systems. *Journal of Petroleum Science and Engineering,* (2003) 39, 389-398.

Bona, N., Rossi E., Venturini C., Capaccioli S., Lucchesi M. and Rolla P.A., Characterization of rock wettability through dielectric measurements, revue de l'Institut Fraincais du Petrole, (1998) 53 771-783.

Borysenko, A.; Clennell, B.; Sedev, R.; Ralston, J.; Raven, M.; Dewhurst, D., Wettability measurements in model and reservoir shale systems. *International Symposium of the Society of Core Analysts, Trondheim (Norway 12-16 September* 2006), SCA2006-03, 1-12.

Clennell, B., Borysenko, A., Dewhurst, D.N., Sedev, R.; Ralston, J.; Liu, K. and Wark, I., Wettability characterization and non-invasive monitoring of effect of crude oil treatment on cap-rock shale minerals. *International Symposium of the Society of Core Analysts, Calgary (Canada 10-12 September* 2007), SCA2007-04, 1-12.

Djurhuus, K., Lien, J.R., Skauge, A. and Sørland, G.H. Measuring wettability from brine T_2 distributions in the presence of an inert mineral oil *International Symposium of the Society of Core Analysts, Trondheim (Norway 12-16 September* 2006), SCA2006-04 1-12

Fleury, M. and F. Deflandre, Quantitative evaluation of porous media wettability using NMR relaxometry, *Magnetic Resonance Imaging*, (2003) 21, 385-387

Garrouch, Ali A., Sharma, Mukul M., The influence of clay content, salinity, stress, and wettability on the dielectric properties of brine-saturated rocks; 10 Hz to 10 MHz, Geophysics, (1994) 59, 909-917.

Looyestijn, W., and Hofman, J. Wettability Index determination by Nuclear Magnetic Resonance. (2005) SPE 93624

Nguyen B.L., Bruining, J., Evert, C. and Slob, E.C. Effects of wettability on dielectric properties of porous media, (1999), SPE 56507.

Song, C., Hou, L., Saini, A. K., and Hatcher, P. G., CPMAS and DDMAS ^{13}C NMR analysis of coal liquefaction residues, American Chemical Society Division of Fuel Chemistry Preprints, (1994**)** 39, 782-786.

Zhang, G. Q.; Huang, C.-C.; Hirasaki, G. J., Interpretation of wettability in Sandstones with NMR Analysis. *Petrophysics* (2000), 41, 223-233.

APPENDIX – FIGURES

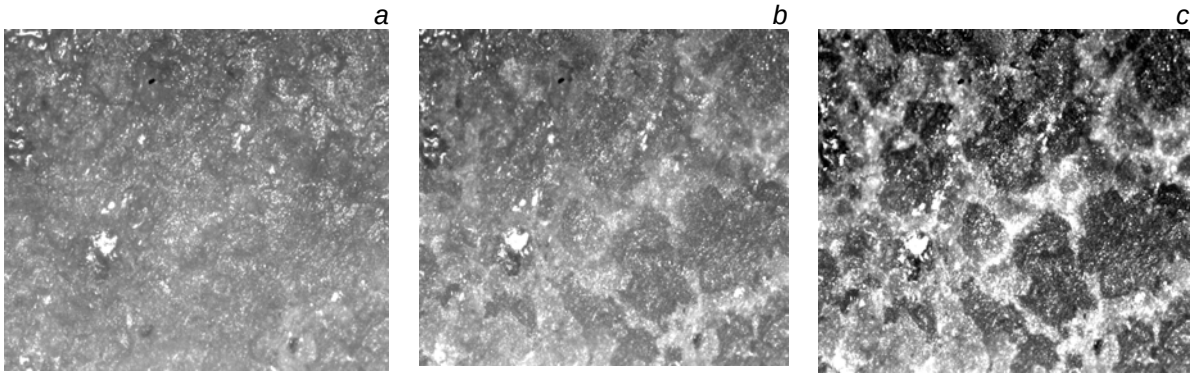

Fig. 1. Optical microscope imaging formation of micro-cracks after hydration of crude oil treated shale a) 10 sec; b) 30 sec; c) 60 sec.

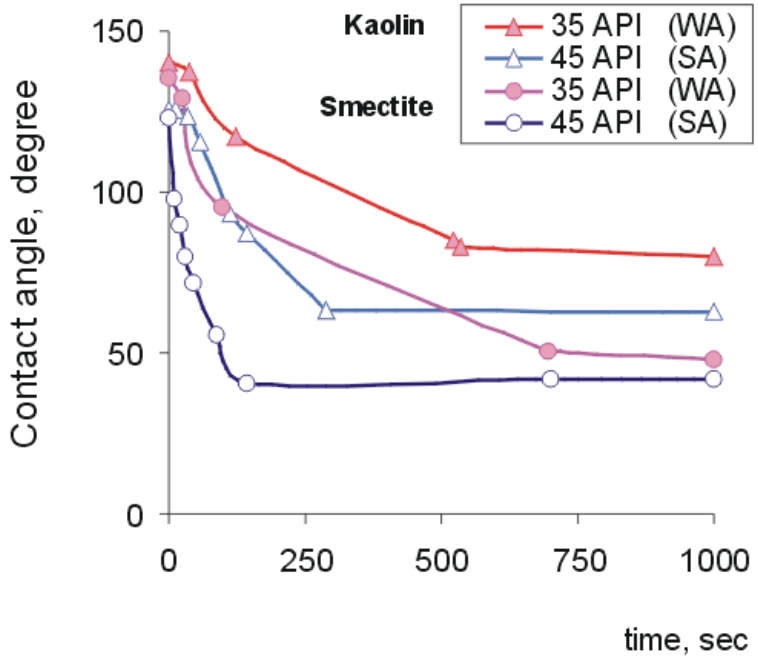

Fig. 2. Decrease over time of contact angle value as a result of breaking the original film and leading to slaking and swelling of the underlying shale.

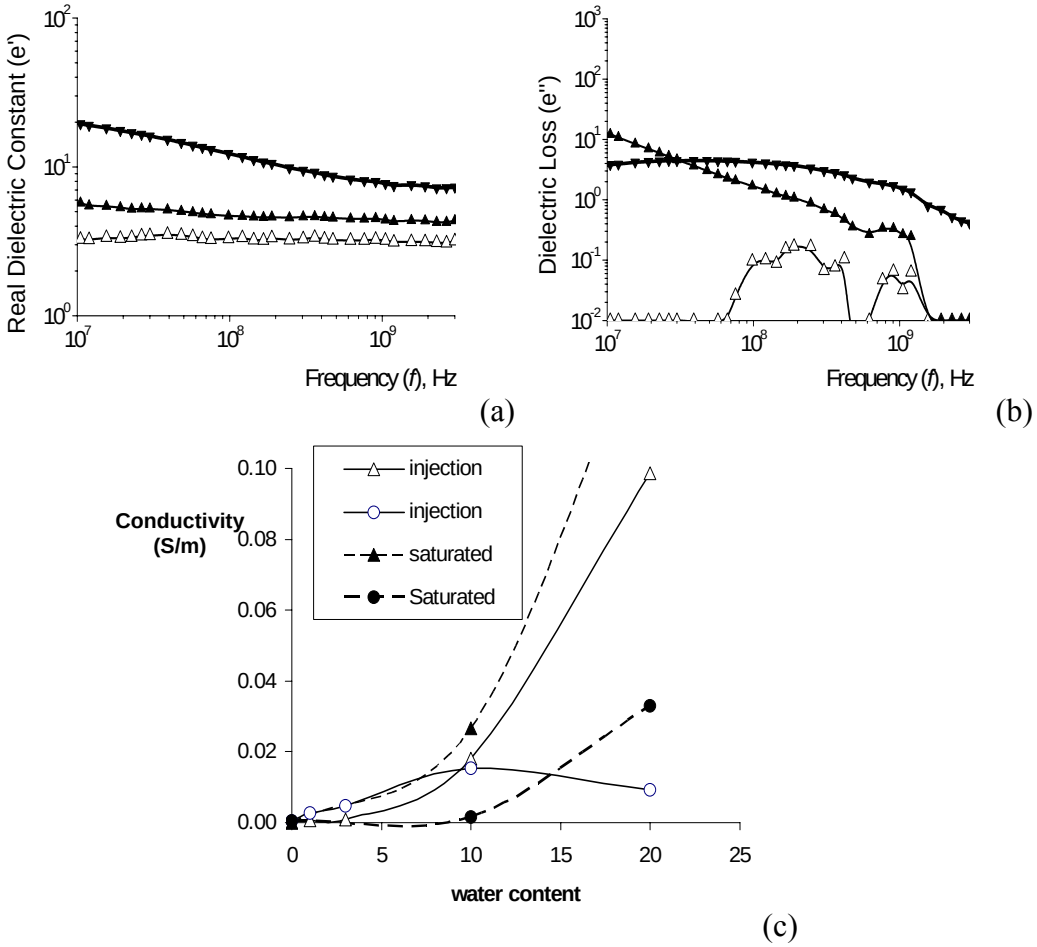

Fig. 3. Real (a) and imaginary (b) part of the dielectric constant of quartz powder: Open triangles – sample treated in crude oil, solid up triangles – after initial water saturation (5 %) and solid down triangles after full saturation. (c) Conductivity (at 10 MHz) as a function of water content for hydrophobic shale (O1AC) and hydrophilic shale (L1_390C).

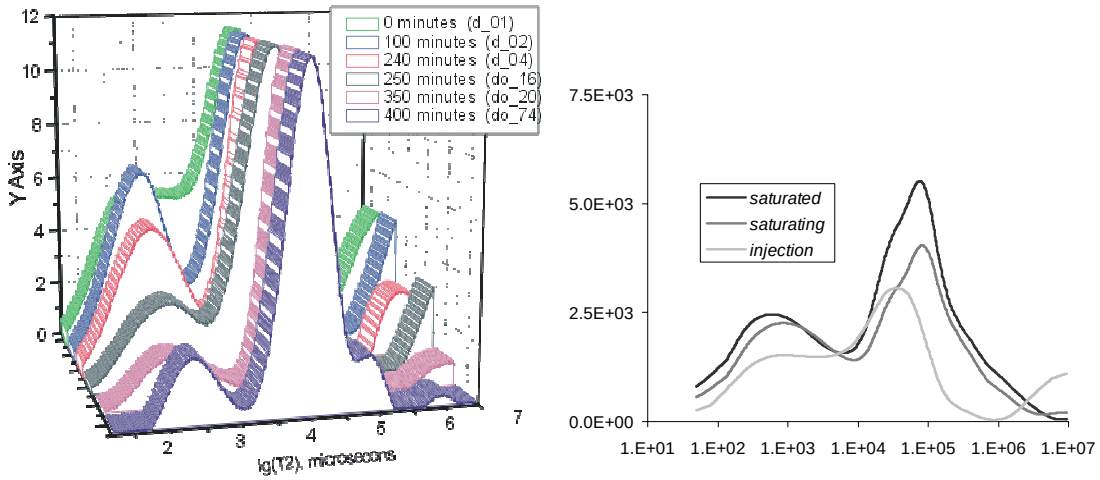

(a) (b)

Figure 4. Proton T_2 distribution measured in 2 MHz Maran spectrometer for model mineral systems. (a) Time lapse measurements of T_2 using the CPMG pulse sequence are a simple way to monitor oil-water displacements and fluid rearrangements. Sequence of fluid injection steps into cleaned quartz first saturating with water by spontaneous imbibition (0-240 minutes) and then with forced imbibition by oil (240-400 minutes). (b) NMR spectra of mixed mineral sample (90% qtz + 10% smectite) undergoing progressive water injection. Clay-bound water and intergranular pore water peaks are distinct.

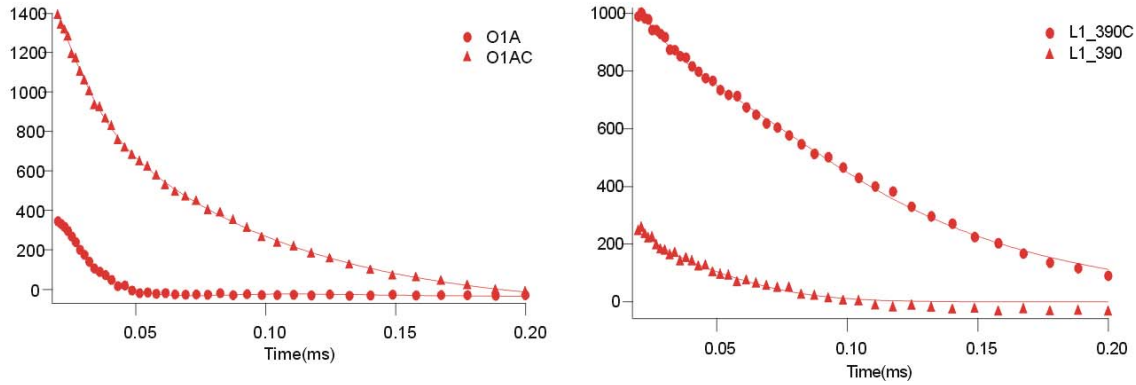

(a) (b)

Fig 5. Minispec proton resonance Solid Echo data for two different shales untreated (lower curves) and aged in oil (upper curves). (a) hydrophobic shale O1A; (b) hydrophilic shale L1_390. The time scale is time after the first pulse in the two pulse solid echo sequence. Vertical scale is signal amplitude in arbitrary units.

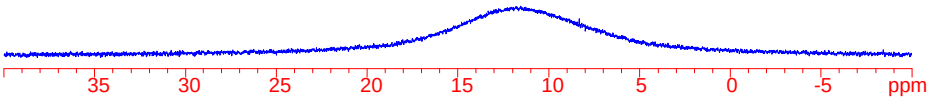

(a)

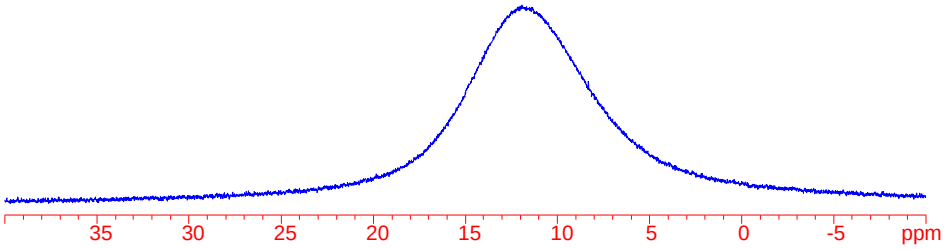

(b)

Figure 6. The proton broad line spectrum of clean quartz (a) and methylated quartz (b). Signal amplitude is relative; both (a) and (b) at same vertical scale.

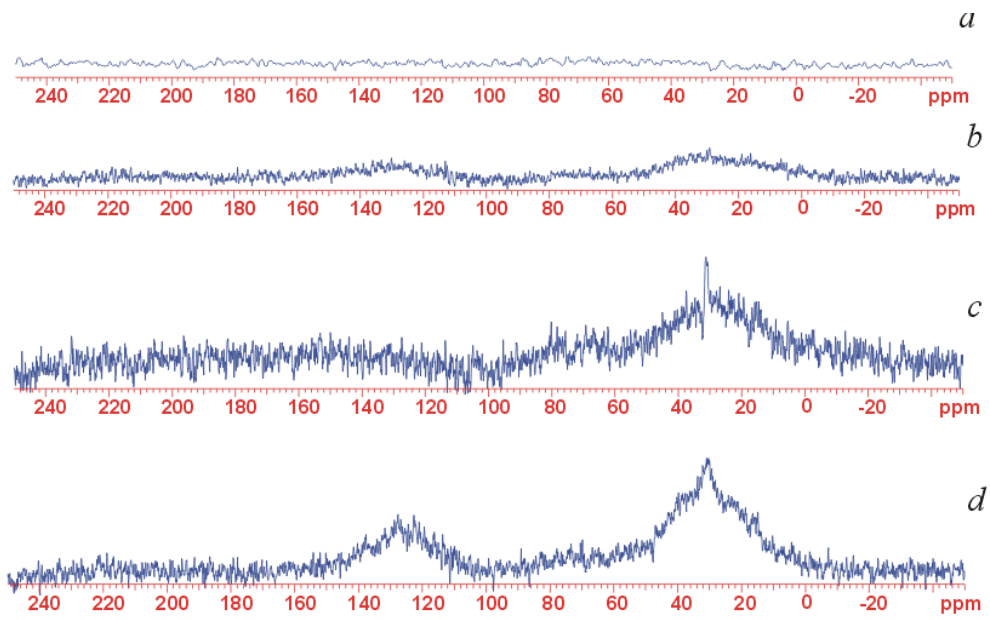

Fig. 7. The carbon CPMAS spectra of a) L1_390 and b) O1A before crude oil treatment. c) LI390C and d) O1AC. after crude oil treatment. Signal amplitude is normalised; all plots shown at same vertical scale.

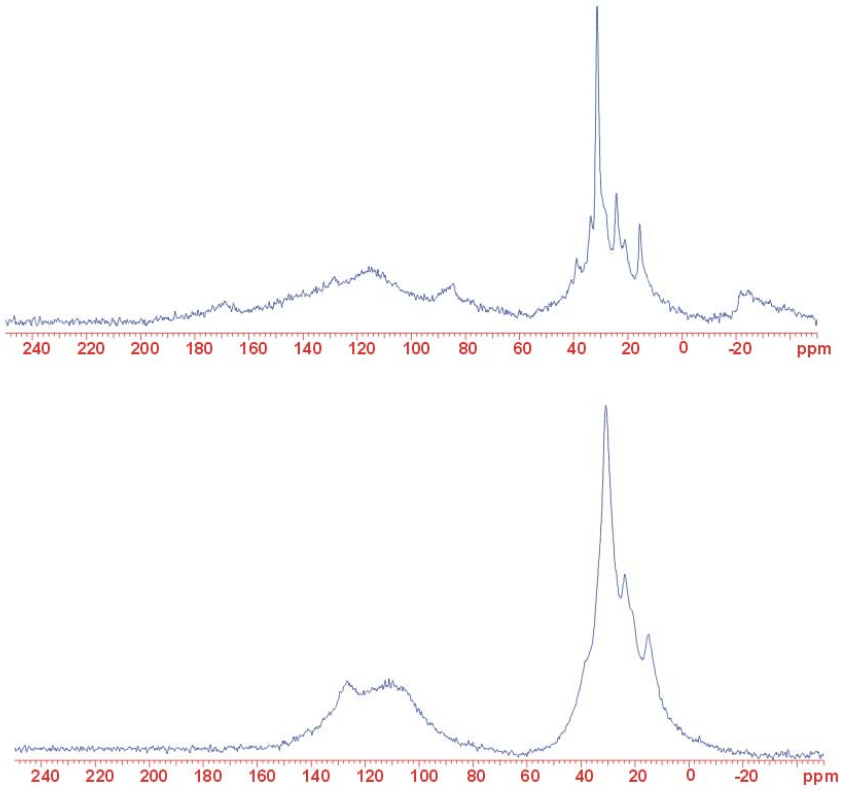

(a)

(b)

Fig. 8. The carbon DDMAS spectra of crude treated L1_390C (top) and O1A (bottom). Signal amplitude is relative; both () and (b) have same vertical scale.